Electrochemical Studies on Uranyl(VI) Species in 1-Butyl-3-methylimidazolium Based Ionic Liquids and Their Application to Pyro-Reprocessing and Treatment of Wastes Contaminated with Uranium

Yasuhisa Ikeda[1], Noriko Asanuma[2] and Yusuke Ohashi[3]
[1]Research Laboratory for Nuclear Reactors, Tokyo Institute of Technology,
[2]Department of Energy Science and Engineering, Tokai University,
[3]Ningyo-toge, Environment Engineering Center, Japan Atomic Energy Agency,
Japan

1. Introduction

Room temperature ionic liquids (ILs) have been paid attention as environmentally benign media, because they have attractive properties such as thermal stability, nonflammability, high ionic conductivity, and wide electrochemical potential windows (Earle & Seddon, 2000; Rogers et al., 2000; Wasserscheid & Welton, 2003). In the nuclear industry field, ILs are expected to be applied as media for reprocessing of spent nuclear fuels and treatment of radioactive wastes contaminated with radioactive nuclides (Bladley et al., 2002; Rogers et al., 2002; Giridhar et al., 2006; Cocalia et al., 2006; Giridhar et al., 2007; Binnemans, 2007).
In this chapter, our feasibility studies on applications of ILs as the media of pyro-reprocessing processes and the treatment method of radioactive wastes contaminated with uranium will be introduced.

2. Investigation on application of ILs as media of the pyro-reprocessing processes

We studied electrochemical properties of uranyl species in 1-butyl-3-methylimidazolium (BMI) based ILs (BMICl, $BMIBF_4$, and BMINfO (NfO = nonafluorobutanesulfonate)) to examine their feasibility as alternatives to conventional molten salts as media for pyro-reprocessing processes for spent nuclear fuels.
BMICl (Kanto Chemical Co., Inc.) was used without further purification and $BMIBF_4$ (Kanto) was purified by using activated carbon. BMINfO was synthesized as follows: 1-Butyl-3-methylimidazole was dissolved into tetrahydrofuran (THF) and stirred vigorously. After that, 1-buromo butane was dropped slowly with a dropping funnel, and the resulting solution was refluxed. After refluxing, THF phase was separated and stirred with ethylacetate (EA). Crude 1-butyl-3-methylimidazolium bromide (BMIBr) was obtained by removing THF and EA *in vacuo*. The crude BMIBr was dissolved into distilled water and

stirred vigorously. To this solution, KNfO was added. The resulting solution was refluxed with stirring at 70 ˚C. The BMINfO phase was separated from aqueous one and mixed with activated carbon for removing organic impurities. After filtration, the filtrate was mixed with the distilled water for striping inorganic impurities. In order to remove water and volatile impurities, all ILs used were kept for more than 3 h under reduced pressure at 120 ˚C.

Sample solutions for electrochemical experiments were prepared by dissolving $Cs_2UO_2Cl_4$ or $UO_2Cl_2{\cdot}nH_2O$ (n = 1~3) into ILs. $Cs_2UO_2Cl_4$ and $UO_2Cl_2{\cdot}nH_2O$ (n = 1 ~ 3) were synthesized according to the reported procedures (Cordfunke, 1969; Denning et al., 1979). Cyclic voltammograms (CV) of sample solutions controlled at appropriate temperatures were measured by using an electrochemical analyzer (BAS, ALS model 660B) in glove box under an Ar atmosphere. A glassy carbon and a Pt wire were used as a working electrode and a counter electrode, respectively. As a reference electrode, an Ag/AgCl electrode was used and connected with a cyclic voltammetry cell by a liquid junction filled with $BMIBF_4$ or BMINfO. All potentials reported here are *vs.* Ag/AgCl. In the CV measurements, potential was swept to cathodic direction initially.

2.1 Electrochemical study on uranyl chloride in BMICl

Figure 1(a) shows the UV-visible absorption spectrum of the solution prepared by dissolving $Cs_2UO_2Cl_4$ into BMICl at 80˚C. This absorption spectrum is found to exhibit remarkable vibrational fine structure, which is similar to that of $[UO_2Cl_4]^{2-}$ in $AlCl_3$/EMIC (EMIC = 1-ethyl-3-methylimidazolium chloride) (Dai et al., 1997), $BMITf_2N$, $MeBu_3NTf_2N$, and C_4minTf_2N (Tf_2N = bis(trifluoromethanesulfonyl)imide, $MeBu_3N$ = tri-*n*-butylmethyl-ammonium, C_4min = 1-hexyl-3-methylimidazolium) (Sornein et al., 2006; Nockemann *et al.*, 2007). Nockemann et al. have reported that the fine structure is typical for the $[UO_2Cl_4]^{2-}$ with D_{4h} coordination symmetry (Nockemann et al., 2007). The molar absorption coefficient (ε) at 429.8 nm (maximum peak) is 14.5 M^{-1} cm^{-1} (M = mol dm^{-3}), and is almost same as those reported previously (Sornein et al., 2006; Nockemann et al., 2007). We also measured the UV-visible absorption spectrum of the solution obtained by dissolving $UO_2Cl_2{\cdot}nH_2O$ in BMICl at 80 ˚C (see Fig. 1(b)), where the concentration of uranium was determined by ICP-AES. A similar absorption spectrum to that in Fig. 1(a) was observed. The ε value of maximum peak at 428.6 nm was 16.3 M^{-1} cm^{-1}. These results indicate that the uranyl species in solutions prepared by dissolving $Cs_2UO_2Cl_4$ or $UO_2Cl_2{\cdot}nH_2O$ into BMICl is $[UO_2Cl_4]^{2-}$. Slight differences in the ε values and the wavelength of peak maxima in Fig. 1(a) and (b) might be due to the effects of Cs^+ ions in BMICl system obtained by dissolving $Cs_2UO_2Cl_4$ and residual water in the sample solutions.

Based on spectrophotometric data, to examine the electrochemical behavior of $[UO_2Cl_4]^{2-}$ in BMICl, CVs of the sample solutions prepared by dissolving $Cs_2UO_2Cl_4$ or $UO_2Cl_2{\cdot}nH_2O$ into BMICl (abbreviated as $Cs_2UO_2Cl_4$/BMICl system and $UO_2Cl_2{\cdot}nH_2O$/BMICl system) were measured at 80 ˚C in the potential range of –1.0 ~ –0.4 V at various scan rates (v = 10 ~ 50 mV s^{-1}). A typical result for the $Cs_2UO_2Cl_4$/BMICl system is shown in Fig. 2 (a). As seen from this figure, two peaks corresponding to one redox couple were observed around –0.72 (E_{pc}) and –0.65 V (E_{pa}). The potential differences between two peaks (ΔE_p) are 75 and 81 mV at 10 and 50 mV s^{-1}, respectively, and close to the theoretical value (67 mV) for the reversible one electron transfer reaction at 80 ˚C. Furthermore, the values of (E_{pc} + E_{pa})/2 is constant, –0.687 ± 0.005 V, regardless of v (see Table 1). Similar results were also obtained from the CVs

for the $UO_2Cl_2{\cdot}nH_2O$/BMICl system at 80 ˚C as shown in Fig. 2 (b), that is, one redox couple was observed around –0.73 (E_{pc}) and –0.66 V (E_{pa}), the ΔE_p values are 69 mV at 10 mV/s and 77 mV at 50 mV/s, the values of $(E_{pc} + E_{pa})/2$ is constant, –0.693 ± 0.001 V (see Table 1). From these results, it is suggested that $[UO_2Cl_4]^{2-}$ in BMICl is reduced to $[UO_2Cl_4]^{3-}$ quasi-reversibly and that the formal redox potential (E^o) is –0.690 V in the present system.
Hence, it should be concluded that BMICl is not applicable as the medium of the pyro-reprocessing process, because the uranyl species in BMICl are not reduced to UO_2.

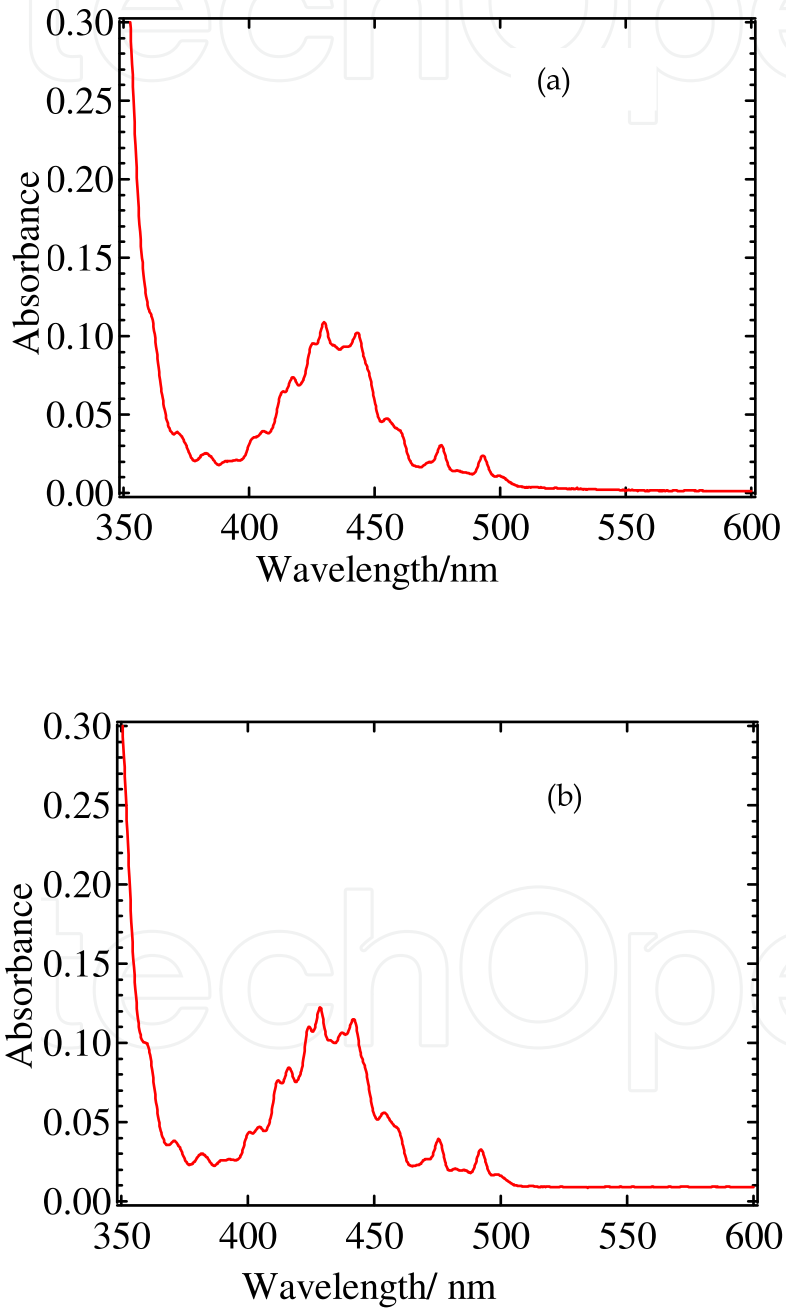

Fig. 1. UV-visible absorption spectra of the solutions prepared by dissolving uranyl chloride complexes into BMICl at 80 ˚C. (a): Complex = $Cs_2UO_2Cl_4$; $[UO_2^{2+}]$ = 1.47 x 10^{-2} M. (b): Complex = $UO_2Cl_2{\cdot}nH_2O$; $[UO_2^{2+}]$ = 1.47 x 10^{-2} M.

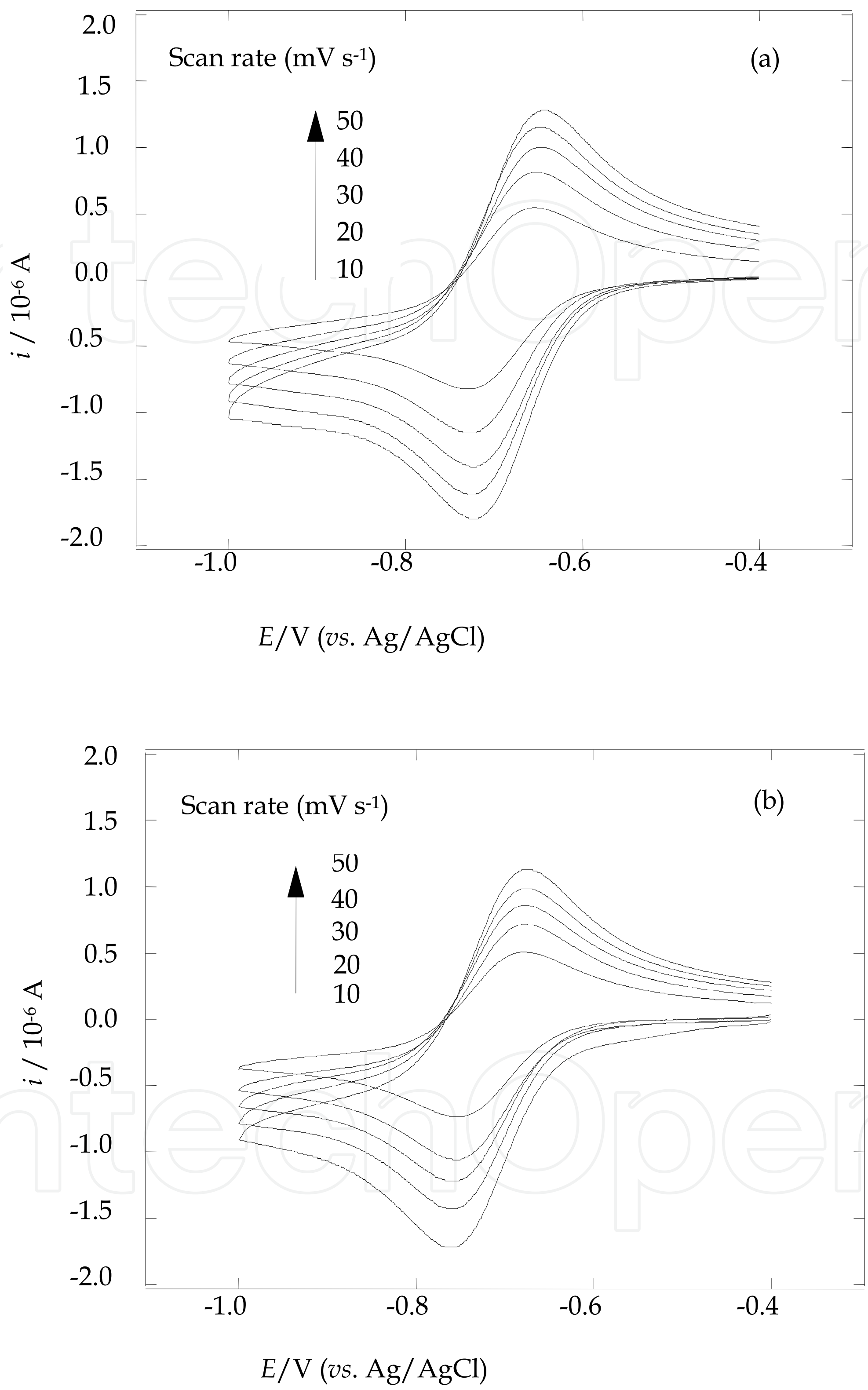

Fig. 2. Cyclic voltammograms of the solutions prepared by dissolving uranyl chloride complexes into BMICl measured in the potential range from –0.1 to –0.4 V at different scan rates (v = 10 ~ 50 mV s^{-1}). (a): Complex = $Cs_2UO_2Cl_4$; [UO_2^{2+}] = 1.47 x 10^{-2} M. (b): Complex = $UO_2Cl_2{\cdot}nH_2O$; [UO_2^{2+}] = 1.47 x 10^{-2} M. Temp. = 80 ˚C. Initial scan direction : cathodic.

System	ν / (mV•s^{-1})	E_{pc} / V	E_{pa} / V	ΔE / V	i_{pc} / A	i_{pa} / A
(a)	10	−0.729	−0.654	0.075	-7.21×10^{-7}	6.59×10^{-7}
	20	−0.727	−0.653	0.074	-1.08×10^{-6}	9.38×10^{-7}
	30	−0.725	−0.646	0.079	-1.32×10^{-6}	1.13×10^{-6}
	40	−0.726	−0.647	0.079	-1.52×10^{-6}	1.29×10^{-6}
	50	−0.723	−0.642	0.081	-1.68×10^{-6}	1.42×10^{-6}
(b)	10	−0.752	−0.682	0.070	-7.36×10^{-7}	4.37×10^{-7}
	20	−0.752	−0.678	0.074	-1.06×10^{-6}	5.95×10^{-7}
	30	−0.754	−0.679	0.075	-1.22×10^{-6}	7.09×10^{-7}
	40	−0.759	−0.679	0.080	-1.43×10^{-6}	8.15×10^{-7}
	50	−0.762	−0.676	0.086	-1.72×10^{-6}	9.18×10^{-7}

(a): $[UO_2^{2+}]$ = 1.47 x 10^{-2} M. (b): $[UO_2^{2+}]$ = 1.47 x 10^{-2} M

Table 1. Cyclic valtammetric data for solutions prepared by dissolving $Cs_2UO_2Cl_4$ (a) and $UO_2Cl_2{\cdot}nH_2O$ (b) into BMICl

2.2 Electrochemical study on uranyl chloride in BMIBF$_4$

Adding $UO_2Cl_2{\cdot}nH_2O$ to BMIBF$_4$, precipitates were formed. Hence, supernatant solutions containing UO_2^{2+} were used for electrochemical experiments. The UV-visible absorption spectrum of supernatant is shown in Fig. 3, and is found to be similar to those of $[UO_2Cl_4]^{2-}$ in Fig. 1. This result suggests that the uranyl species in the supernatant exists as $[UO_2Cl_4]^{2-}$. The CV measurements were continuously repeated five times in the range of –1.0 ~ 1.0 V. The results are shown in Fig. 4. An irreversible reduction peak was observed around −0.7 V and gradually decreased with the repetition of the potential sweep. By wiping off the surface of working electrode, the reduction peak was appeared again. This suggests that the surface of the electrode is covered by insoluble film produced by redox reaction. Similar phenomenon was reported by Chagnes et al., that is, they observed the formation of a blocking film on the graphite electrode in CV measurements in BMIBF$_4$ (Chagnes et al., 2005).

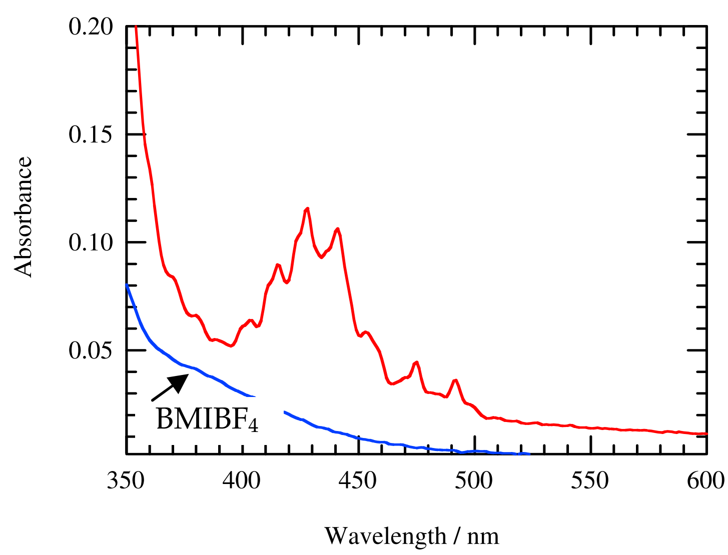

Fig. 3. UV-visible absorption spectrum of the supernatant solution prepared by adding $UO_2Cl_2{\cdot}nH_2O$ into BMIBF$_4$ at 80 ˚C. $[UO_2^{2+}]$ = 5.1x10^{-3} mol/kg.

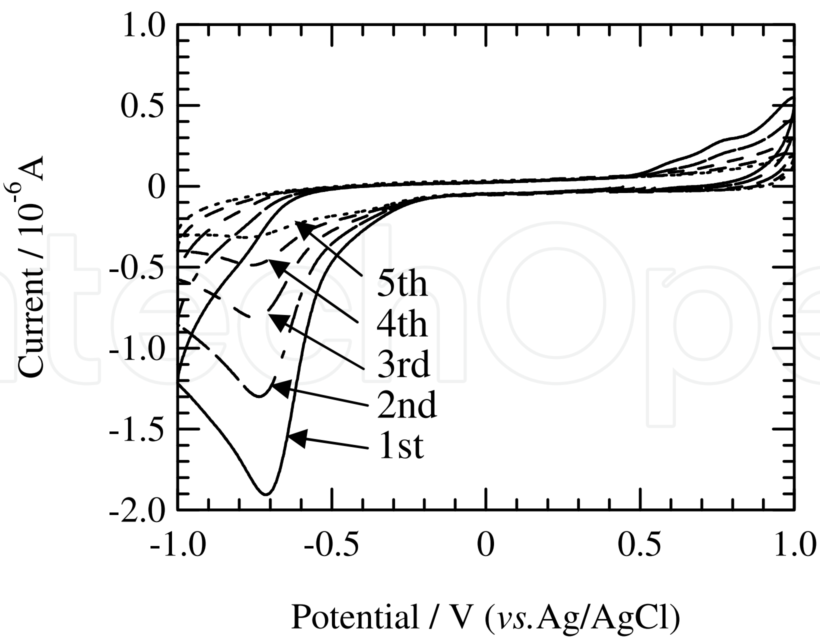

Fig. 4. Cyclic voltammograms of uranyl species in $BMIBF_4$ (80˚C, $[UO_2^{2+}]$ = 5.1x10^{-3} mol/kg, sweep rate = 50 mV/s).

Judging from the above results, $BMIBF_4$ is concluded to be not applicable as the medium of the pyro-reprocessing process.

2.3 Electrochemical study on uranyl chloride in BMINfO

Figure 5 shows the UV-visible absorption spectrum of the solution prepared by dissolving $UO_2Cl_2{\cdot}nH_2O$ into BMINfO at 80˚C. As seen from this figure, the absorption spectrum is different from those of $[UO_2Cl_4]^{2-}$ shown in Fig. 1. Although we do no have exact data on the structure yet, it seems likely that the uranyl species in BMINfO is present as $[UO_2Cl_2(NfO)_n]^{n-}$.

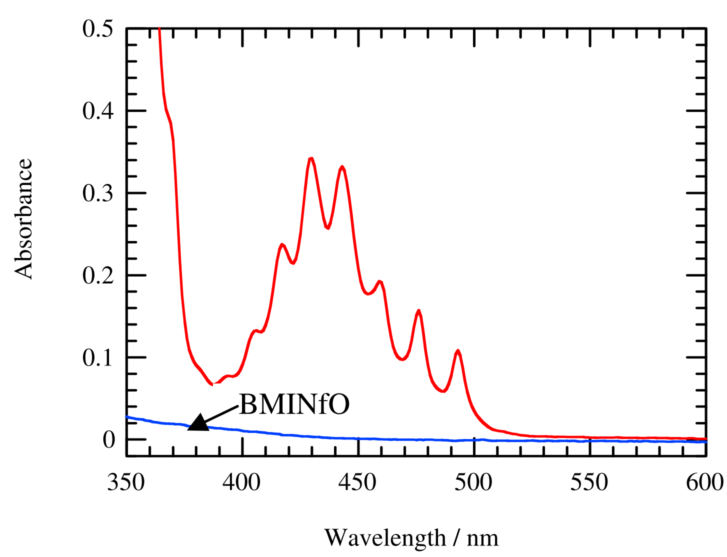

Fig. 5. UV-visible absorption spectrum of the solution prepared by dissolving $UO_2Cl_2{\cdot}nH_2O$ into BMINfO at 80˚C. $[UO_2^{2+}]$ = 8.7 x 10^{-3} mol/kg.

Figure 6 shows CVs of neat BMINfO and uranyl species in BMINfO. As seen from this figure, three irreversible reduction peaks (i, ii, iii) and a sharp oxidation one (iv) appear in the range of −0.6 ~ −0.2 V and around 0.85 V, respectively. It is known that a sharp oxidation peak (iv) is due to the oxidative dissolution of reduction products deposited on the electrode (Shirai et al., 1998). Therefore, the sharp oxidation peak at 0.85 V is considered to corresponds to oxidative dissolution of U(IV) compounds deposited on the electrode. Thus, the reduction peaks should be assigned to multi step reduction of U(VI) to U(IV) as follows.

i. U(VI) + e → U(V)
ii. U(V) + e → U(IV)
iii. U(VI) + 2e → U(IV)

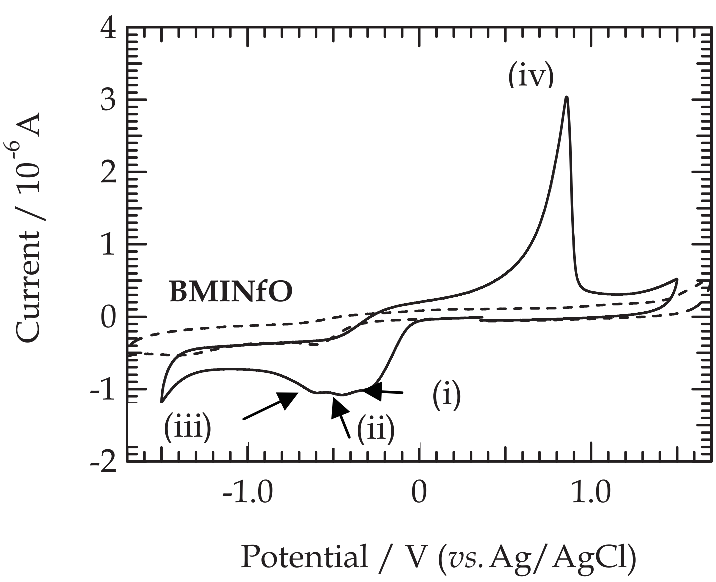

Fig. 6. Cyclic voltammograms of neat BMINfO and uranyl species in BMINfO (80˚C, [UO_2^{2+}] = 8.7 x 10^{-3} mol/kg, sweep rate = 50 mV/s).

2.4 Bulk electrolysis of uranyl species in BMINfO

Judging from the results of the CV measurements described above, it might be possible to recover UO_2 by electrochemical reduction of UO_2^{2+} in BMINfO. Thus, bulk electrolysis of UO_2^{2+} (0.3 mol·kg^{-1}) in BMINfO was carried out at −1.0 V by using cell for bulk electrolysis shown in Fig. 7. As a result, the deposits were produced on a carbon electrode as cathode and a part of such deposits was fallen to the bottom of the electrolysis cell. The photograph of recovered deposits is shown in Fig. 8. After the electrolysis, the IL on the carbon electrode was washed away with acetone and dichloromethane, and then the surface of the carbon electrode was analyzed by the scanning electron microscope (SEM) and the energy dispersive X-ray spectrometer (EDX). The micrograph and distribution of elements on the electrode surface are shown in Fig. 9. The distribution of carbon is attributable to the carbon electrode. Consequently, it was found that the deposits are uranium compounds including chlorine components such as uranium oxides and uranium oxychlorides.

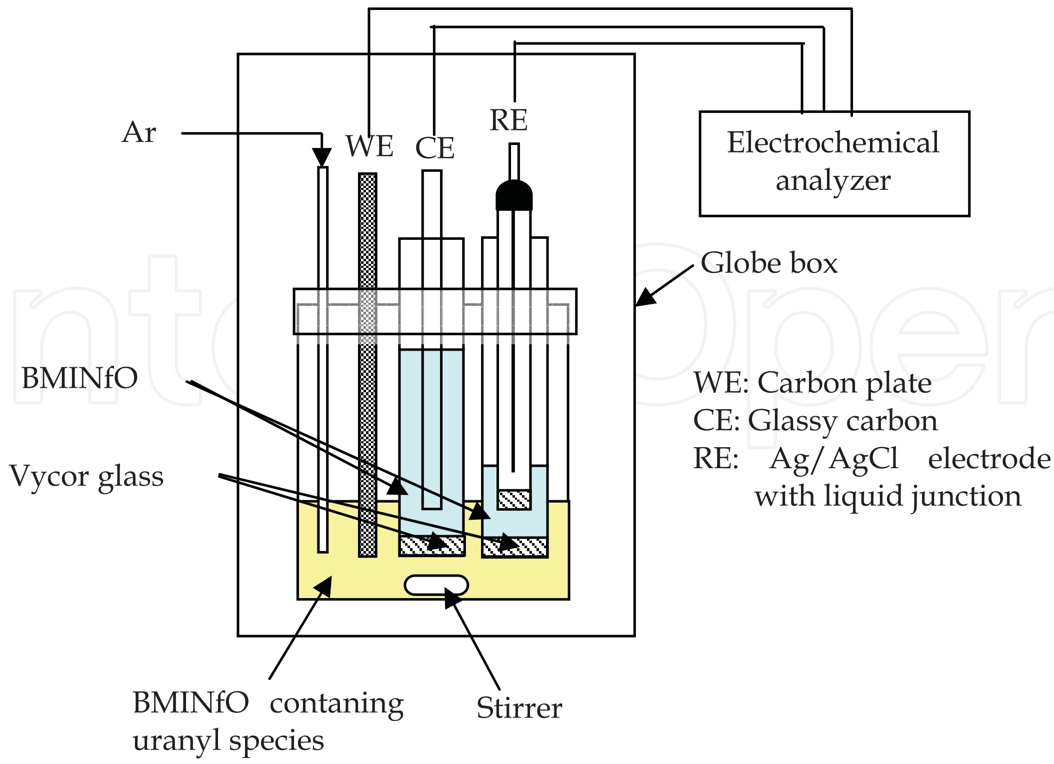

Fig. 7. Cell for bulk electrolysis.

Fig. 8. A photograph of the deposits recovered by electrochemical reduction of uranyl species in BMINfO.

2.5 Summary of electrochemical properties of uranyl species in BMI based ionic liquids

Electrochemical properties of uranyl species in BMICl, $BMIBF_4$, and BMINfO were examined by using cyclic voltammetry. And based on such investigations, the applicability of ILs as the media of pyro-reprocessing processes was also examined. The results are summarized as follows.

- In BMICl, the reversible redox couple was observed in CV. This suggests that the redox couple corresponds to the redox couple of UO_2^{2+}/UO_2^{+} with one electron transfer.
- In $BMIBF_4$, an irreversible reduction peak was observed around −0.7 V and gradually decreased by the repetition of the potential sweep. This phenomenon is caused by the formation of insoluble reduction products on the surface of the electrode.

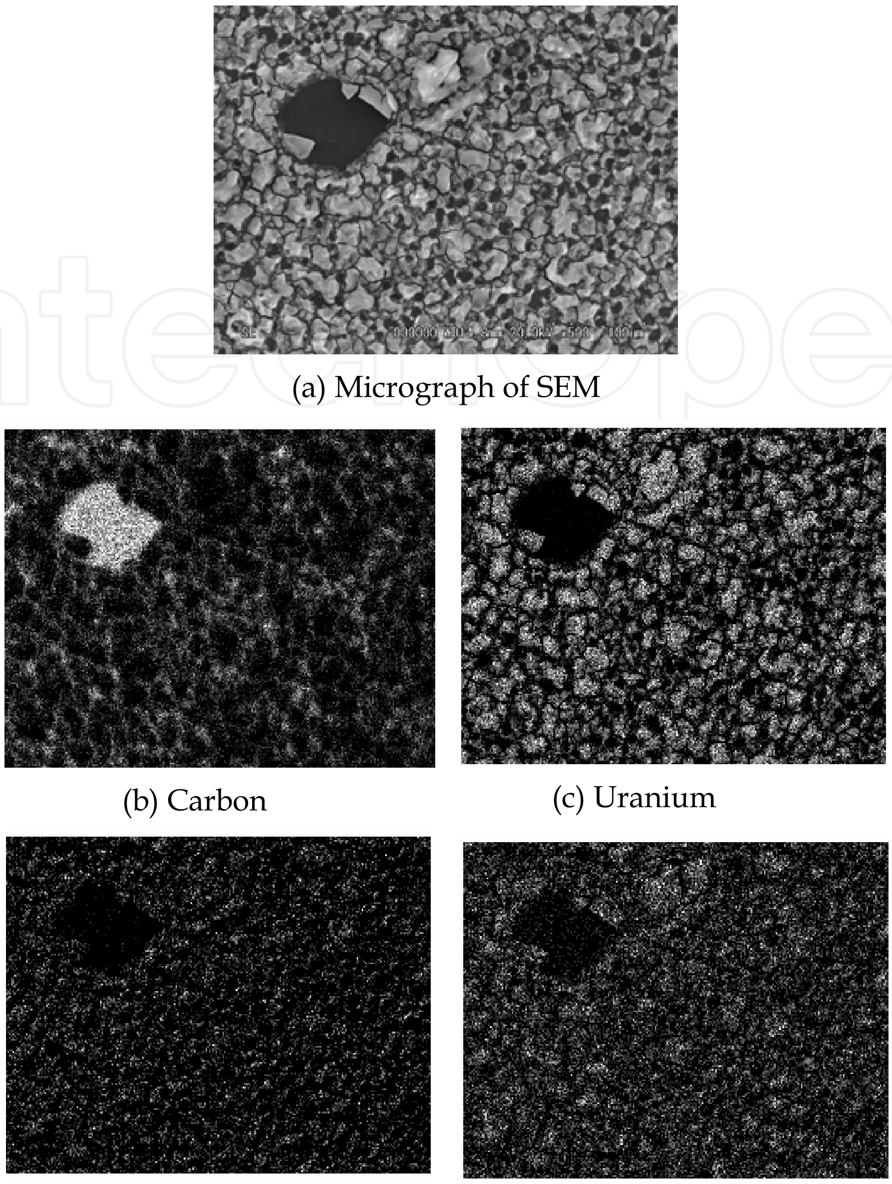

(a) Micrograph of SEM

(b) Carbon (c) Uranium

(d) Oxygen (e) Chlorine

Fig. 9. Micrograph of SEM and distribution of elements analyzed by EDX for the electrode surface after the bulk electrolysis of uranyl species in BMINfO.

- In BMINfO, three irreversible reduction peaks and a sharp oxidation one were observed in the range of −0.6 ~ −0.2 V and around 0.85 V, respectively. This suggests that the redox reactions consist of the multi step reduction of U(VI) to U(IV) and the oxidative dissolution of U(IV) as reduction products.
- Electrochemical reduction of uranyl species in BMINfO was performed by bulk electrolysis. As a result, deposits were observed on the cathodic electrode. From the SEM-EDX analyses, it was confirmed that the deposits are uranium compounds including chlorine components such as uranium oxides and uranium oxychlorides.
- These results indicate that the uranyl species in IL can be recovered electrolytically as uranium compounds. Hence, from the electrochemical viewpoint it is expected that ILs can be used as media of pyro-reprocessing processes.

- A new pyro-reprocessing method shown in Fig. 10 should be proposed. This method consists of three processes, i.e., first one is the dissolution of spent nuclear fuels using oxidant such as Cl_2, second one is the recovery of UO_2 by electrochemical reduction, and third one is the electrochemical deposition of UO_2/PuO_2 mixed oxide.

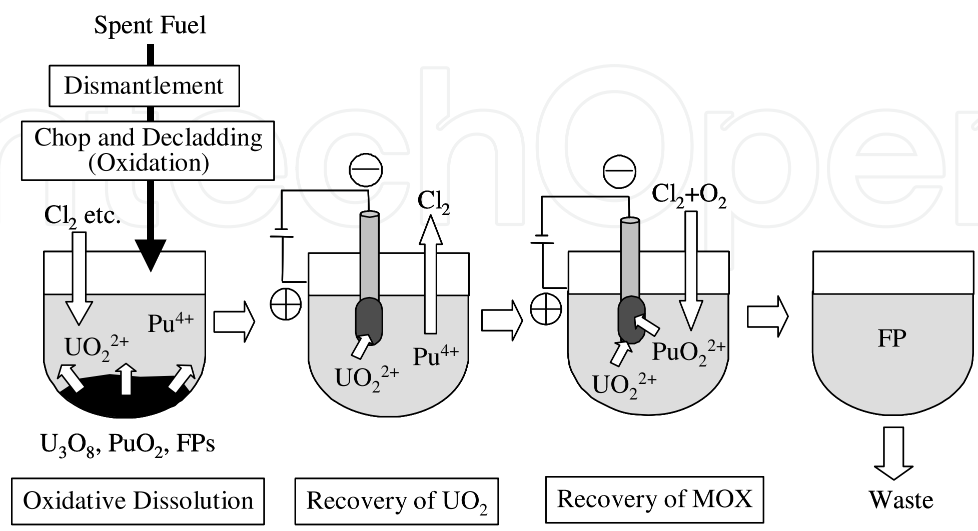

Fig. 10. Schematic diagram of proposed processes of the pyro-reprocessing by using IL as media

3. Investigation on application of ILs as electrolytic media for treating wastes contaminated with uranium

Most of metal and bed materials generated from uranium enrichment facilities or uranium refining and conversion plants are contaminated by uranium fluorides such as UF_4. These wastes are mainly classified as the medium-level wastes. Hence, it is desired to recover uranium as much as possible from such wastes. Moreover, if these wastes are decontaminated up to the clearance level, the resulting decontaminated materials should be reused. As one of effective decontamination methods of metal wastes, wet chemical decontamination processes using inorganic or organic acids have been developed (Ikeda et al., 2002; Enda et al., 2006). However, from such wet processes, a relatively large amount of secondary wastes should be generated with treating spent acid solutions, because base metal part of wastes is dissolved by acid with the dissolution of contaminated part. And also it is reported that uranium of spent adsorbents can be recovered by electrolysis in sodium chloride molten salt (Amamoto et al., 2005). However, this method must be performed under high temperature (672ºC). Decontamination methods carried out under milder conditions must be preferable. Ionic liquids are expected to meet such demands. Hence, we investigated the solubility of UF_4 in ILs and the electrochemical properties of uranium species dissolved into ILs

Uranium tetrafluoride (UF_4) was synthesized from yellow cake according to the reported method (Higgins et al., 1958). Synthesis of UF_4 was confirmed using a X-Ray diffractometer (Rigaku, RAD-rPC). Impurities in UF_4 were detected using an ICP-MS (Thermo electron Co., ELEMENT). Purity of UF_4 was 97 %. BMICl was used as an IL. Water containing BMICl was removed by heating *in vacuo*. Water content in BMICl after drying was determined to be 0.1 wt % using a Karl Fischer moisture content meter (Metrohm, 737 KF Coulometer).

3.1 Dissolution behavior of UF_4 powders

Dissolution experiments were carried out at 100ºC under the atmosphere with stirring at 100 rpm. The UF_4 powders (0.1 g, 3.2×10^{-4} mol) were weighed accurately and dissolved in BMICl solution (1.0 ml) in a beaker. After dissolution, the residual solid phases were filtered off and the uranium concentrations in the filtrates were measured ICP-MS. Figure 11 shows a plot of dissolution ratios *vs*. time. As seen from this figure, the UF_4 powders do not dissolve in BMICl easily.

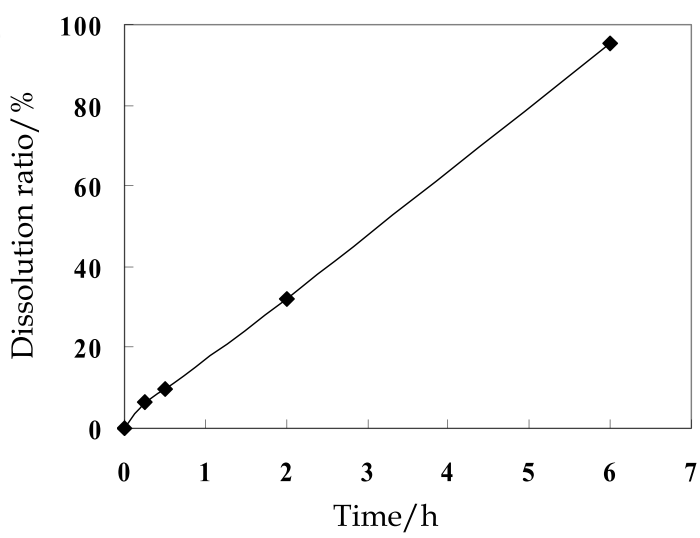

Fig. 11. A plot of dissolution ratios *vs*. time for the dissolution of UF_4 powders (0.1 g) in BMICl (1.0 ml) at 100 ºC.

The color of the dissolution solution was green after about 1 h and the powders were completely dissolved after around 6 h. The color of BMICl solution after complete dissolution of UF_4 was yellowish green. However, its absorption spectrum did not show characteristic bands assigned to the U^{4+} species (Rodden, 1964). The yellowish green solution was further heated for 10 h under the atmosphere. As a result, the color of the solution changed from yellowish green to yellow. Figure 12 shows the absorption spectrum of the resulting solution and is similar to that of $UO_2Cl_4^{2-}$ shown in Fig. 1. The ε value at maximum peak of 422 nm is 13.1 M^{-1} cm^{-1} and almost the same as that (about 14 M^{-1} cm^{-1}) at maximum peak of 429 nm reported (Sornein et al., 2006). This result indicates that the species generated with the dissolution of UF_4 powders are oxidized to uranyl(VI) by O_2 under the present conditions. The relative slow dissolution of UF_4 in BMICl should be due to that the oxidation process of U(IV) with O_2 is slow.

Wipff *et al*. have reported that in BMICl dissolving uranyl triflate (TfO^-) or uranyl perchlorate, Cl^- ions interact with uranyl(VI) more strongly than ClO_4^- and TfO^-, and that the uranyl(VI) species mainly exist as $UO_2Cl_4^{2-}$ (Gaillard et al., 2007). And also they have proposed from the results of molecular dynamics (MD) and quantum mechanical (QM) calculations that F^- ions coordinate to uranyl(VI) more strongly than Cl^-(Gaillard et al., 2007; Chaumont & Wipff, 2005). Based on these reports, it is suggested that the uranyl(VI) species with the mixed ligands of F^- and Cl^- should be formed in the BMICl solution dissolving UF_4.

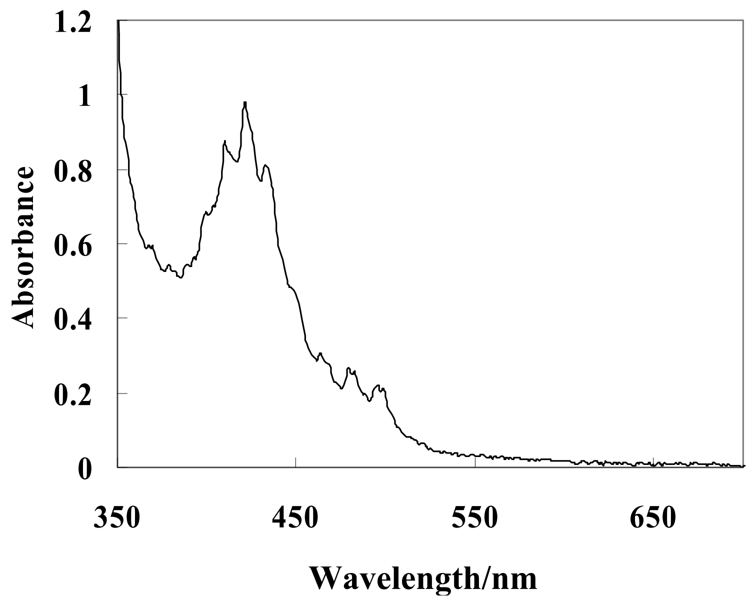

Fig. 12. UV-visible absorption spectrum of the solution prepared by dissolving UF_4 into BMICl ($[UO_2^{2+}]$ = 8.0 x 10^{-2} M)

3.2 Elecrochemistry of sample solutions prepared by dissolving UF_4 into BMICl

The cyclic voltammograms of the sample solutions prepared by dissolving UF_4 (0.52 g) into BMICl (30 ml) were measured at 80 °C in the potential range -2.0 – 0.95 V at 50 mV/s. In these experiments, a glassy carbon wire, a Pt wire, a Ag/AgCl electrode (BAS, RE-1B) with a liquid junction filled with BMICl were used as working, counter, and reference electrode, respectively. The result is shown in Fig. 13. As seen from this figure, one uncoupled reduction peak and one uncoupled oxidation peak are observed around -0.93 and 0.18 V, respectively, and the current value of the oxidation peak is smaller than that of the reduction peak. This result is different from that of $Cs_2UO_2Cl_4$ system mentioned in 2.1. In the BMICl system dissolving $Cs_2UO_2Cl_4$, the uranyl(VI) species were confirmed to be present as $UO_2Cl_4^{2-}$, and one quasi-reversible redox couple assigned as $UO_2Cl_4^{2-} + e^- = UO_2Cl_4^{3-}$ was observed around -0.72 and -0.65 V. These support the above suggestion that the uranyl(VI) species with the mixed ligands of F^- and Cl^- are formed in the BMICl solution dissolving UF_4, and suggest that the reduction product of the uranyl(VI) complexes with the mixed ligands of F^- and Cl^- are less stable than that of $UO_2Cl_4^{2-}$, *i.e.*, $UO_2Cl_4^{3-}$. Sornein et al. have reported that the uncoupled reduction peak should correspond to the following reduction processes (Sornein et al., 2006).

$$\text{Uranyl(VI)} + e^- \rightarrow \text{Uranyl(V)}$$

$$\text{Uranyl(V)} + e^- \rightarrow UO_2$$

From these results, it is expected that the uranium component can be recovered electrolytically from the solutions generated in the decontamination treatments of the wastes contaminated with UF_4 in BMICl.

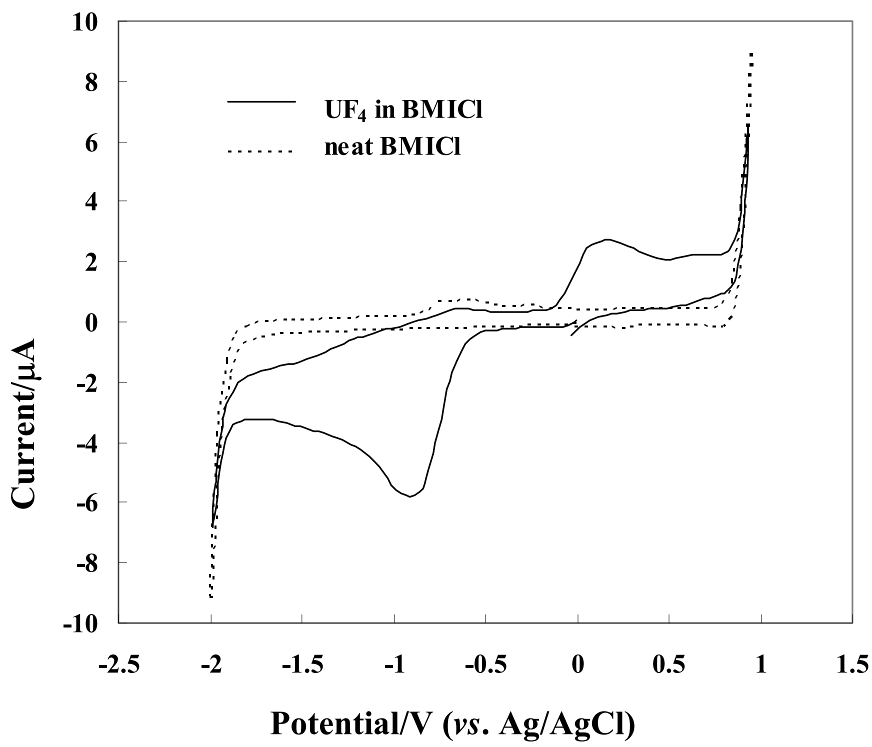

Fig. 13. Cyclic voltammograms of the solution prepared by dissolving UF_4 in BMICl ($[UO_2^{2+}]$ = 8.0×10^{-2} M) and neat BMICl at 80 °C. Initial scan direction: cathodic.

3.3 Application to decontamination of the steel wastes contaminated with uranium

Samples of steel waste were prepared from the dismantled carbon steel cylinders which had been used for storing UF_6 (see Fig. 14). The chemical forms of uranium species adhered on the steel wastes were confirmed to be UF_4 by measuring XRD. Chemical forms of iron species on surfaces of contaminated steel wastes were confirmed to be FeF_3 and Fe_2O_3 by X-ray Photoelectron Spectroscopy (JEOL, JPS-9000MC) using Mg Kα radiation of 1253.6 eV.

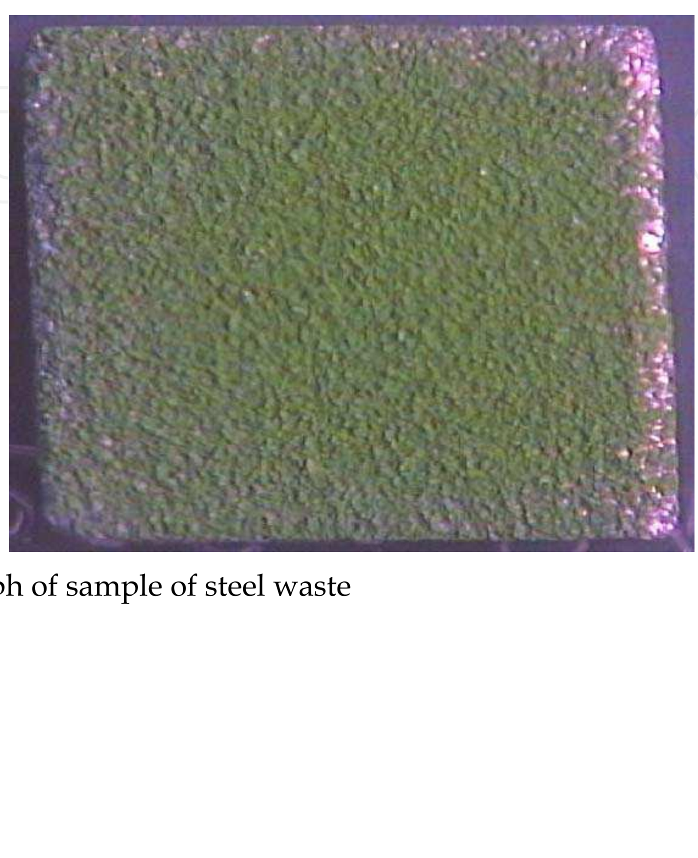

Fig. 14. A photograph of sample of steel waste

The contaminated steel wastes were cut into the quarter sector (28mm Φ × 6 mm thick, central angle 90°), and soaked in BMICl (2.0 ml) at 100 °C under the atmosphere. After decontamination, the ILs remained on surfaces of steel wastes were washed off with ethanol. Uranium concentrations (Bq/g) of decontaminated steels were evaluated as the ratio of radioactivity due to U of samples to total weight of samples.
Figure 15 shows a plot of U concentrations (Bq/g) against time in the dissolution of adhered uranium by soaking the contaminated steel waste into BMICl. The U concentrations are found to drop below the temporary proposed clearance level (1.0 Bq/g) within 3 h under the present conditions (IAEA, 2004).

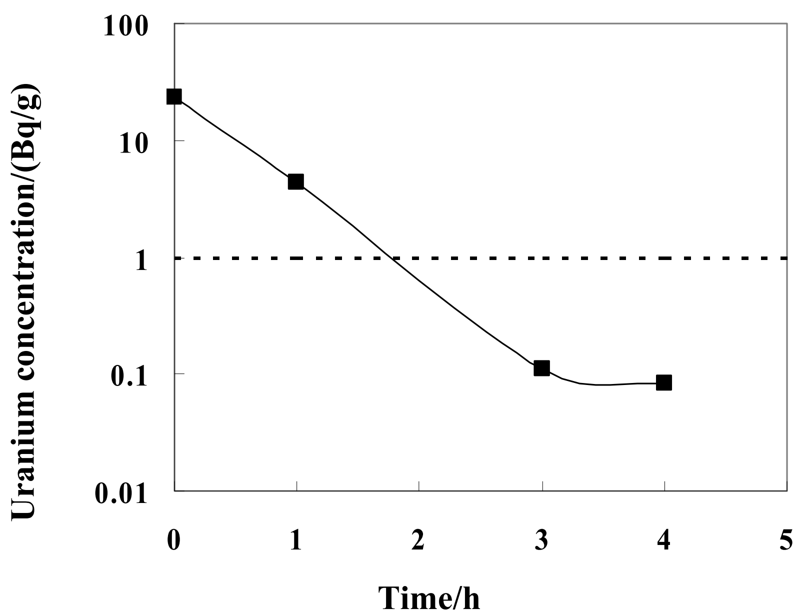

Fig. 15. A plot of uranium concentrations of steel waste *vs*. soaking time for the dissolution in BMICl at 100 °C under the atmosphere

Furthermore, the XPS spectra for the top surface of the steel waste were measured after decontamination treatment. As a result, the peaks due to UF_4 and FeF_3 were found to disappear. This indicates that the FeF_3 component is also dissolved with the dissolution of UF_4 in BMICl.
As mentioned in 3.2, it is suggested that the uranium component can be recovered electrolytically from the BMICl solution dissolving UF_4. Hence, it should be possible to recover only uranium component from the solutions after decontamination of the steel wastes in BMICl by controlling electrolytic potential.

3.4 Summary for application of ILs to the treatment of wastes contaminated with uranium

Dissolution behaviour of UF_4 in BMICl and the electrochemical properties of dissolved uranium species were investigated. Based on such basic studies, the feasibility of decontamination of steel wastes contaminated uranium using BMICl as medium was also examined. The results are summarized as follows.

- UF_4 can be dissolved completely in BMICl by heating under the atmosphere.

- From the UV-visible absorption spectra of dissolution solutions, it was found that the dissolved uranium species are oxidized to uranyl(VI) by O_2 and that the resulting uranyl(VI) species are the complex with the mixed ligands of F^- and Cl^-.
- The CV measurements suggest that the resulting uranyl(VI) species with the mixed ligands of F^- and Cl^- are reduced to UO_2 electrochemically.
- The steel wastes contaminated with UF_4 can be decontaminated below the temporarily proposed clearance level (1.0 Bq/g) within 3 h by soaking in BMICl at 100 ^oC.
- It should be possible to recover only uranium component from the solutions after decontamination of the steel wastes in BMICl by controlling electrolytic potential.

4. References

Earle, K.J.; Seddon, K.R. (2000). Ionic liquids. Green solvents for the nature. *Pure Appl. Chem.*, 72, 1391-1398

Rogers, R.D.; Seddon, K.R.; Volkov, S. (2000). *Green Industrial Applications of Ionic Liquids*, Kluwer Academkic Publishers, Dordrecht

Wasserscheid, P. & Welton, T. (2003). *Ionic Liquids in Synthesis*, Wiley-VCH, Weinheim

Bradley, A.E.; Hatter J.E.; Nieuwenhuyzen, M.; Pinter, W.R.; Seddon, K.R. & Thied, R.C. (2002). Precipitation of a dioxouranium(VI) species from a room temperature ionic liquid medium. *Inorg. Chem.*, 41, 1692-1694

Rogers, R.D. & Seddon, K.R. (2002). *Ionic Liquids: Industrial Applications to Green Chemistry,* ACS Symposium Series 818, American Chemical Society, Washington, DC

Giridhar, P.; Venkatensan, K.A.; Subramaniam, S.; Srinivasan, T.G. & Rao, P.R.V. (2006). Electrochemical behaviour of uranium(VI) in 1-butyl-3-methylimidazolium chloride and in 0.05 M aliquat-336/chloroform. *Radiochim. Acta*, 94, 415-420

Cocalia, V.A.; Gutowski, K.E. & Rogers, R.D. (2006). The coordination chemistry of actinides in ionic liquids: a review of experiment and simulation. *Coord. Chem. Rev.*, 250, 755-764

Giridhar, P.; Venkatesan, K.A.; Srinivasan, T.G. & Rao, P.R.V. (2007). Electrochemical behavior of uranium(VI) in 1-butyk-3-methylimidazolium chloride and thermal characterization of uranium oxide deposit. *Electrochim. Acta*, 52, 3006-3012

Binnemans, K. (2007). Lanthanides and actinides in ionic liquids. *Chem. Rew.*, 107, 2592-2614

Cordfunke, R.G. (1969). *The Chemistry of Uranium*, Elsevier Publishing Co., Amsterdam

Denning, R.G.; Snellgrove, T.R. & Woodwork, D.R. (1979). The electronic structure of uranyl ion Part I. The electronic spectrum of $Cs_2UO_2Cl_4$. *Mol. Phys.*, 32, 419-442

Dai, S.; Shin, Y.S.; Toth, L.M. & Barnes, C.E. (1997). Comparative UV-Vis studies of uranyl chloride complex in two basic ambient-temperature melt systems: the observation of spectral and thermodynamic variations induced via hydrogen bonding. *Inorg. Chem.*, 36, 4900-4902

Sornein, M.-O.; Cannes, C.; Naour, C.L.; Langarde, G. ; Simoni, E. & Berthet, J.-C. (2006). Uranyl complexation by chloride ions. Formation of a tetrachlorouranium(VI) complex in room temerature ionic liquids [Bmim][Tf_2N] and [$MeBu_3N$][Tf_2N]. *Inorg. Chem.*, 45, 10419-10421

Nockemann, P.; Servaes, K.; Deun, R.V.; Hecke, K.V.; Meervelt, L.V.; Binnemans, K. & Walrand, C.G. (2007). Speciation of uranyl complexes in ionic liquids by optical spectroscopy. *Inorg. Chem.*, 46, 11335-

Chagnes, A.; Diaw, M.; Carré, B.; Willmann, P.; Lemordant, D. (2005). Immidazolium-organic solvent mixtures as electolytes for lithium batteries. J. Power Sources, 145, 82- 88

Shirai, O.; Iwai, T.; Suzuki, Y.; Sakamura, Y.; Tznaka, H. (1998). Electrochemical behavior of actinide ions in LiCl-KCl eutectic melts. *J. Alloys Com.*, 271-273, 685-688

Ikeda, A.; Aida, M.; Fujii, Y.; Kataoka, S.; Annen, S. & Sato, J. (2002). Ion exchange separation for decontamination of centrifuge enrichment plant. *J. Nucl. Sci. Technol.*, 39, 1099-1105

Enda, M.; Sato, T.; Sakai, H.; Natsui, K. & Ishikura, T. (2006). Development of chemical decontamination technique using formic acid. *Trans. At. Energy Soc. Japan*, 15, 364-373

Amamoto, I.; Terai, T.; Oobayashi, H. & Fujita, R. (2005). Separation and recovery study of uranium from spent NaF (fillers). *J. Phys. Chem. Solids*, 66, 602-607

Higgins, I.R.; Robert, J.T. & Hancher, C.W. (1958). *Ind. Eng. Chem.*, 50, 285-292

Rodden, C.J. (1964). *Analysis of Essential Nuclear Reactor Materials*, U.S.A.E.C., GPO, Washington, D.C.

Gaillard, C.; Chaumont, A.; Billard, I.; Hennig, C, Ouadi, A. & Wipff, G. (2007). The competition between ionic liquid anions, uranyl counterions, and Cl- anions investigated by extended X-ray absorption fine structure and UV-visible spectroscopies and molecular dynamics simulations. *Inorg. Chem.*, 46, 4815-4826

Chaumoun, A. & Wipff, G. (2005). Solvation of fluoro and mixed fluoro/chloro complexes of Eu^{III} in the [BMI][PF_6] room temperature ionic liquid. A theoretical study. *Phys. Chem. Chem. Phys.*, 7, 1926-1932

International Atomic Energy Agency. (2004). *Application of the concepts of exclusion, exemption and clearance*, IAEA Safety Standards Series, No. RS-G-1.7

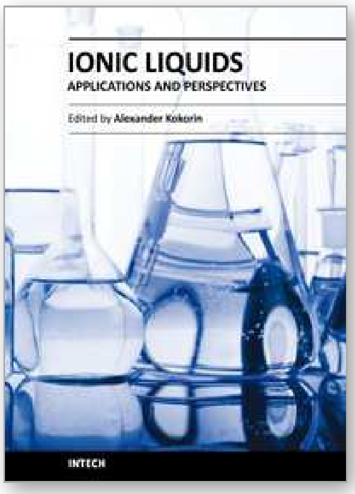

Ionic Liquids: Applications and Perspectives

Edited by Prof. Alexander Kokorin

ISBN 978-953-307-248-7
Hard cover, 674 pages
Publisher InTech
Published online 21, February, 2011
Published in print edition February, 2011

This book is the second in the series of publications in this field by this publisher, and contains a number of latest research developments on ionic liquids (ILs). This promising new area has received a lot of attention during the last 20 years. Readers will find 30 chapters collected in 6 sections on recent applications of ILs in polymer sciences, material chemistry, catalysis, nanotechnology, biotechnology and electrochemical applications. The authors of each chapter are scientists and technologists from different countries with strong expertise in their respective fields. You will be able to perceive a trend analysis and examine recent developments in different areas of ILs chemistry and technologies. The book should help in systematization of knowledges in ILs science, creation of new approaches in this field and further promotion of ILs technologies for the future.